J Mol Model (2013) 19:2391–2397
DOI 10.1007/s00894-013-1786-z

ORIGINAL PAPER

Molecular dynamics simulation on miscibility of trans-1,4,5,8-tetranitro-1,4,5,8 -tetraazadecalin (TNAD) with some propellants

Li Xiao-Hong · Zhao Feng-Qi · Xu Si-Yu · Ju Xue-Hai

Received: 23 November 2012 / Accepted: 28 January 2013 / Published online: 15 February 2013

Abstract The solubility parameters of TNAD, HMX, RDX, DINA, DNP propellants were predicted by molecular dynamics (MD) simulation in order to evaluate the miscibility of TNAD and the other four propellants. The results show that the order of miscibility is TNAD/DINA > TNAD/DNP > TNAD/RDX > TNAD/HMX from the analysis of miscibility. The densities and binding energies of TNAD/propellants blends were further investigated. The results indicate that the better the miscibility between TNAD and the propellants, the smaller the variation of the density rate. The larger the intermolecular interaction, the better the miscibility between components. The analysis of radial distribution function shows that the main interaction ways between TNAD and other energetic components are short-range interactions.

Keywords Compatibility · Molecular dynamics simulation · Solubility parameter · Trans-1,4,5,8-tetranitro-1,4,5,8-tetraazadacalin (TNAD)

Electronic supplementary material The online version of this article (doi:10.1007/s00894-013-1786-z) contains supplementary material, which is available to authorized users.

L. Xiao-Hong (✉) · J. Xue-Hai (✉)
Department of Chemistry, Nanjing University of Science and Technology, Nanjing 210094, People's Republic China
e-mail: lorna639@126.com
e-mail: xhju@njust.edu.cn

L. Xiao-Hong
College of Physics and Engineering, Henan University of Science and Technology, Luoyang 471023, People's Republic China

Z. Feng-Qi · X. Si-Yu
Laboratory of Science and Technology on Combustion and Explosion, Xi'an Modern Chemistry Research Institute, Xi'an 710065, China

Introduction

Compatibility is an important safety aspect related to the production and storage of energetic materials. The incompatibility between the energetic material and other components may accelerate the aging and alter the thermal stability of the energetic material itself, impairing the safety and functionality of the entire system. Therefore, the compatibility of an explosive, as well as pyrotechnics and propellants should be investigated carefully before they are used with safety in technical applications [1]. The physical compatibility is also named as miscibility and is the mutual solubility between the components of propellants or explosives. The solubility parameter δ and interaction parameter can be used to characterize the miscibility of the system [2]. The solubility parameter provides a numerical estimate of the degree of interaction between materials, and can be a good indication of solubility. Molecular interaction strength essentially determines the compatibility of multicomponent system. For two components system formed by intermolecular force, larger binding energy is beneficial to their miscibility.

The explosive trans-1,4,5,8-tetranitro-1,4,5,8-tetraazadacalin (TNAD) is an energetic compound containing two fused piperazine rings, which can be used as a main ingredient in cast explosives and propellants [3–5]. It is identified as a promising high energy density material (HEDM) with low shock sensitivity and good thermal stability. Qiu et al. [6] have theoretically studied the structural and electronic properties of TNAD. Prabhakaran et al. [7] studied the kinetics and mechanism of thermal decomposition of TNAD. Skare [8] studied the thermal behavior of nitroamine including TNAD.

Recently, Yan et al. [9] have studied the compatibility of TNAD with some energetic components by using the differential scanning calorimetry (DSC) method. In their study,

the DSC method evaluated the compatibility according to the difference of decomposition peak temperature T_p of the energetic material and the binary system. This is to say that the discharged quantity of gas is a criterion of the compatibility. So the compatibility stated by Yan et al. [9] is the chemical compatibility.

The miscibility of TNAD with some energetic components is one of the most important aspects in practical applications. However, there are no theoretical reports on these aspects. Therefore, our objective is to theoretically investigate the miscibilities between TNAD with some commonly used energetic materials such as cyclotetramethylenetetranitroamine (HMX), cyclotrimethylenetrinitramine (RDX), dinitropiperazine (DNP) and N-nitrodihydroxyethylaminedinitrate (DINA) by using the COMPASS forcefield based molecular dynamics (MD) techniques.

Computational details

Molecular modeling process of physical model

Using Amorphous cell module of the software Materials Studio [10], the amorphous cells of pure TNAD, HMX, RDX, DNP and DINA were constructed, respectively. In order to reduce size effect and not to make too much computation, all the constructed models consist of about 1000 atoms. At 298 K and 1.01×10^5 Pa, the experimental densities of TNAD, HMX, RDX, DNP and DINA are 1.74 [11], 1.9 [12], 1.81 [13], 1.53 [14] and 1.67 g/cm^3 [12].

Four blending amorphous cells were also constructed. Each blending amorphous cell consists of about 1700 atoms. The mass ratios of TNAD to HMX, RDX, DNO and DINA are all 1:1, which are consistent with the experiment by Yan et al. [9]. The initial densities are obtained according to the additivity of volume ratio for TNAD/HMX, TNAD/RDX, TNAD/DNP and TNAD/DINA blends. Because of configurational diversity, ten different amorphous cells were constructed as the object of the next investigation for each blending and pure systems. Table 1 lists the molecular number of each blending and pure systems. Figure 1 gives the molecular structures and numbering of TNAD, HMX, RDX, DNP and DINA.

Simulation details

Condensed-phase optimized molecular potential for atomistic simulation studies (COMPASS) is a powerful force field that supports atomistic simulations of condensed phase materials. The force field enables accurate and simultaneous prediction of structural, conformational, vibrational and thermophysical properties which exist for organic molecules, inorganic small molecules, and polymers in isolation and in condensed phases, and under a wide range of conditions of temperature and pressure [15–17]. Bunte et al. [18] investigated the mechanical and other condensed phase properties of energetic materials using COMPASS force field. In addition, the force field is used to compute the properties of a variety of molecules containing the nitrate ester functionality. Excellent agreement has been obtained between the calculated and experimental values for the studied properties. Cui et al. [19] investigated the phase transitions and mechanical properties of HMX by molecular dynamics simulation and COMPASS force field was used.

In this paper, the geometrical optimization was performed on the constructed amorphous cells by using smart minimization method and COMPASS force field [16]. Using smart minimization method, the constructed amorphous molecular models were optimized.

The MD simulations were carried out in normal pressure and temperature (NPT) with Andersen thermostat method [20] and Berendsen barostat method [21] to control the system pressures and temperatures. The initial molecular speed is Maxwell distribution sampling and solved using velocity Verlet algorithm [22]. The long-range nonbond Coulombic and van der Waals interactions were managed using Ewald method [23] and atom-based summation method [24], respectively. The cutoff distance was 12.5 Å, spline width was 1.00 Å and buffer width was 0.5 Å. A fixed time step of 1 fs was used in all MD simulations. At each temperature and pressure, amorphous states were built using the cubic unit cells subjected to periodic boundary conditions. Simulations were performed with the Discover MD simulation modules. Systems were first relaxed for 50 ps in the equilibration run, followed by a production run of 200 ps. The data from the production run were collected to compute the solubility parameter, density, binding energy

Table 1 The molecular number of each blending and pure systems

Pure amorphous cells	Molecular number	Blending amorphous cell	Molecular number
TNAD	40	TNAD/HMX	28/30
HMX	45	TNAD/RDX	28/40
RDX	60	TNAD/DNP	22/40
DNP	60	TNAD/DINA	28/36
DINA	50		

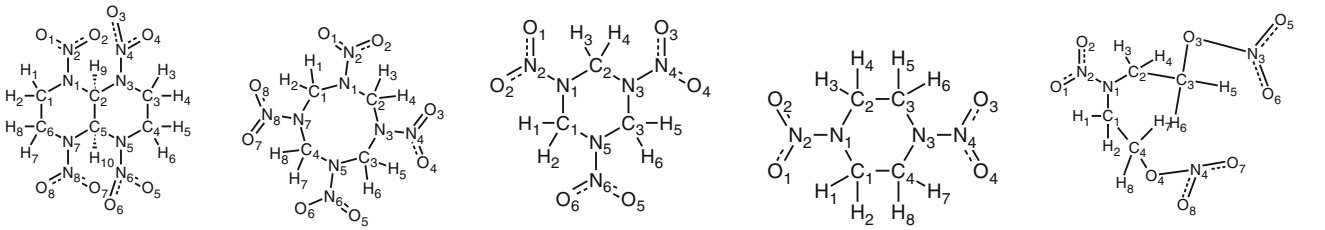

Fig. 1 The molecular structures of TNAD, HMX, RDX, DNP and DINA

and radial distribution functional. Equilibrium criterion is that the standard deviation of temperature is less than 15 K and energy fluctuates along a constant value. Figure 2 shows that the profiles of temperature-simulation time and energy-simulation time of the pure TNAD system.

The theoretical analysis of miscibility of TNAD with HMX, RDX, DNP and DINA

When two materials blend, the compatible thermodynamic condition is as follows:

$$\Delta G_M = \Delta H_M - T\Delta S_M < 0, \tag{1}$$

where ΔG_M, ΔH_M, ΔS_M are mixing free energy, mixing heat and mixing entropy, respectively. For a blending system, ΔH_M is always greater than zero if there is not interaction between different molecules. The increase of mixing entropy is limited for the mixing of the blending materials in propellants [25], so ΔG_M is determined by the ΔH_M value. Hildebrand et al. [26] introduced the concept of solubility parameter and defined it as the square of cohesive energy.

$$\delta = \sqrt{\frac{\Delta E}{V}} = \sqrt{\frac{\Delta H_v - RT}{V}}, \tag{2}$$

where ΔE, V and ΔH_V are the internal energy, volume and vaporization heat, respectively.

The relationship [2] between the mixing heat and solubility parameter of system is

$$\frac{\Delta H_M}{V} = (\delta_1 - \delta_2)^2 \varphi_1 \varphi_2 \tag{3}$$

where φ_1 and φ_2 are the volume fraction of components 1 and 2, respectively. Obviously, the closer the solubility parameters of two components, the better the miscibility. So the solubility parameter can be used to predict the miscibility of different components.

Results and discussion

Validation of the COMPASS force field

Before carrying out the calculations here, we applied the COMPASS force field to TNAD, HMX, RDX, DINA and DNP. The calculated bond lengths and angles were given in Table 2 together with the experimental data. The bond lengths and angles calculated by DFT B3LYP/6-311++G** method were also listed in Table 2. In addition, the charges from the COMPASS for the molecules shown in Fig. 1 were listed in Supporting information Table S1.

Generally, it is found that the bond lengths and angles computed by COMPASS forcefield and DFT method are all closer to the experimental values for

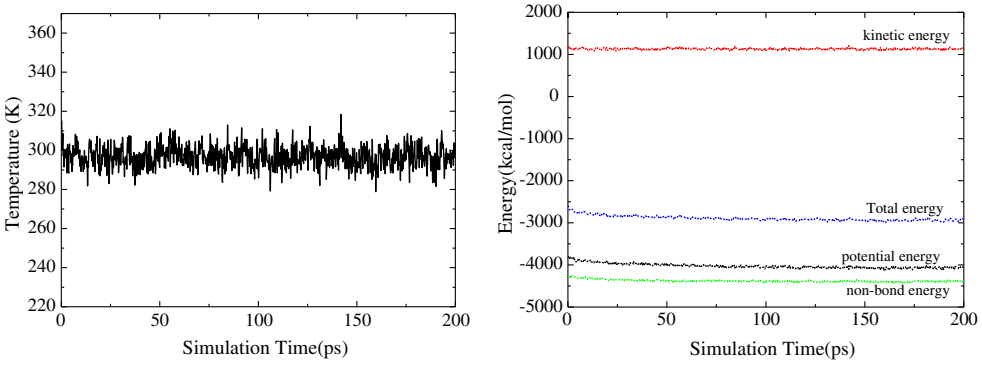

Temperature vs. Simulation Time

Energy vs. Simulation Time

Fig. 2 Profiles of temperature-simulation time and energy-simulation time of pure TNAD system

Table 2 Bond lengths and angles for TNAD, HMX, RDX, DINA and DNP with experimental results by COMPASS forcefield and DFT B3LYP/6-311++G** method

Compds	Methods	C1-N1	C2-N1	N1-N2	N3-N4	C1-N1-N2	C1-N1-C2
TNAD	COMPASS	1.460	1.480	1.400	1.407	119.100	113.969
	DFT	1.4786	1.4798	1.411	1.4213	117.5	111.03
HMX	COMPASS	1.456(1.450)[a]	1.452(1.43)	1.396(1.410)	1.394(1.370)	119.19(117.3)	122.073(124.3)
	DFT	1.479	1.4528	1.4008	1.3918	118.4566	123.3926
RDX	COMPASS	1.453(1.467)[b]	1.448(1.443)	1.395(1.392)	1.392(1.391)	116.956(116.6)	118.408(119.723)
	DFT	1.4603	1.4604	1.4231	1.4224	118.1428	115.8245
DINA	COMPASS	1.474	1.471	1.416	1.4102	119.574	113.503
	DFT	1.4673	1.463	1.438	1.3872	116.3411	112.3673
DNP	COMPASS	1.480	1.480	1.407	1.407	116.93	114.00
	DFT	1.4658	1.4658	1.3991	1.3991	116.0177	115.3826

[a] Data from ref [26]

[b] Data from ref [27]

HMX and RDX. Some computed bond lengths and angles by COMPASS force field are even closer to the experimental values than those computed by DFT B3LYP/6-311++G** method. This shows that the COMPASS force field is suitable for the energetic materials studied in the work. The computed values by DFT method for TNAD, DNP and DINA were also listed in Table 2.

The prediction of the solubility parameter for TNAD with some energetic materials

Table 3 gives the computational solubility parameters of pure materials and the solubility parameters predicted by group contribution method. δ_{VK} was obtained by van Krevelen parameters [28]. Table 4 lists the $\Delta\delta$ values obtained by different methods. Research [2] indicates that two components are compatible when $|\Delta\delta| < (1.3 \sim 2.1)\ J^{1/2} \cdot cm^{-3/2}$ if there is no strong polar group or hydrogen bond interaction. From Table 4, it is noted that $|\Delta\delta_{MD}|$ values of TNAD/DINA and TNAD/DNP are 0.007 and 0.653, respectively. For TNAD/RDX and TNAD/HMX systems, $|\Delta\delta_{MD}|$ values are 2.451 and 2.501, respectively. This shows that TNAD/RDX and TNAD/HMX systems are incompatible and TNAD/DINA and TNAD/DNP systems are compatible.

In addition, in order to validate our computation, we computed the solubility parameters of DINA and TNAD for different cutoffs 10.5, 12.5, 15.5 Å. The computational results were listed in Supporting information Table S2. Obviously, the obtained $|\Delta\delta|$ is closer to the result by van Krevelen parameters when the cutoff is 12.5 Å, which validates our computation.

The experimental results [9] show that TNAD/RDX system is compatible and TNAD/DNP is incompatible, while our computational results show that TNAD/RDX system is incompatible and TNAD/DNP is compatible. The reason is that only the miscibility is considered in our computation. Physical change happens in the components of the system, which includes the changes of mutual penetration or migration, the density and strength of the components of system. However, the experimental test of compatibility for the TNAD/energetic component

Table 3 Solubility parameter δ ($J^{1/2}/cm^{-3/2}$) calculated using MD method

System	δ_{MD}[b]	δ_{VK}[a]
TNAD	22.301	21.23
HMX	24.802	25.34
RDX	24.752	22.64
DNP	21.648	22.10
DINA	22.294	21.37

[a] δ_{VK} is obtained using the Hansen approach and the parameters tabulated by van Krevelen and Hoftyzer [21]. [a] δ_{MD} is obtained using the MD simulation results

Table 4 $\Delta\delta$ ($J^{1/2}/cm^{-3/2}$) calculated using various approaches

Blends	$\lvert\Delta\delta_{MD}\rvert$	$\lvert\Delta\delta_{VK}\rvert$
TNAD-HMX	2.501	4.11
TNAD-RDX	2.451	1.41
TNAD-DNP	0.653	0.87
TNAD-DINA	0.007	0.14

$|\Delta\delta_{MD}|$, $|\Delta\delta_{VK}|$ are differences between solubility parameter values of TNAD and other energetic components

binary systems was carried out by the DSC method [9] and the experimental result is the outcome of chemical compatibility.

According to our results, the order of miscibility is TNAD/DINA > TNAD/DNP > TNAD/RDX > TNAD/HMX. From Table 5, we can see that the $|\Delta\delta_{MD}|$ values of TNAD/RDX and TNAD/HMX are closer because of the similar structures of RDX and HMX. In addition, the order of miscibility is consistent with the order by van Krevelen parameters, which shows that our computational results are reliable.

The relationship between the miscibility and density

For comparison, we took TNAD/DINA and TNAD/HMX for examples and gave the conformation change of blend before and after MD simulations (see Fig. 3). Before MD simulation, the components of system distribute uniformly. After 150 ps MD simulation, the components of the system have stronger interaction for TNAD/DINA system, and the volume of blending becomes smaller and the density becomes larger. However, for TNAD/HMX system, after MD simulation, the volume becomes larger and the density becomes smaller. The density change rate is defined as follows:

$$\beta = \frac{\rho_{before} - \rho_{after}}{\rho_{before}} \times 100\% \quad (4)$$

Table 5 listed the density change rates of systems before and after MD simulation. From Table 5, the order of density change rates is TNAD/DNP > TNAD/HMX > TNAD/RDX > TNAD/DINA. This shows that the better the miscibility between TNAD and other energetic materials, the smaller the density change rate.

The relationship of the binding energy and the miscibility

The interaction among the components directly influences the mechanical strength and sensitivity of the system [2]. In addition, the physical, chemical and explosive properties are all related with their aggregation state and molecular interaction [2, 29]. The intermolecular interaction energy or the intermolecular binding energy (ΔE) can quantitatively characterize the strength of intermolecular interaction [30–34].

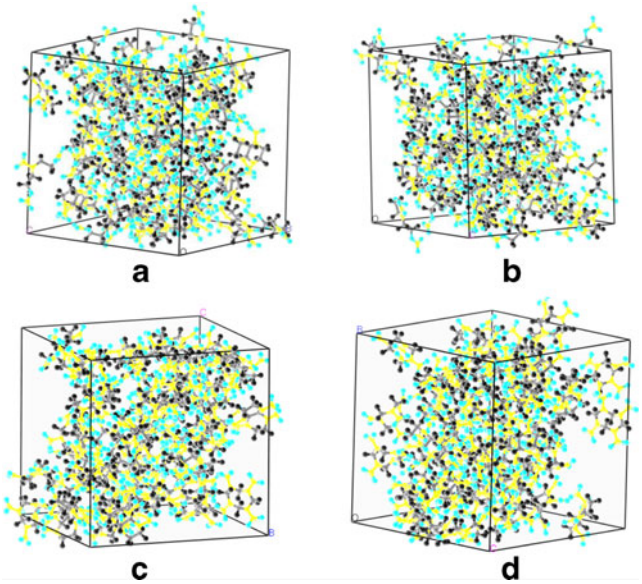

Fig. 3 The conformation changes of blend before and after MD simulation (conformation of TNAD/DINA before (**a**) and after (**b**) MD simulation, conformation TNAD/HMX before (**c**) and after (**d**) MD simulation)

The intermolecular interaction energy ΔE can be calculated as follows:

$$\Delta E = E_{total} - E_{TNAD} - E_{energetic\ material}, \quad (5)$$

where E_{total} is the total energy of the blending system. Table 6 listed the energy of each pure component and the interaction energy of TNAD with some energetic components.

It is noted that the binding energies of the TNAD/DNP and TNAD/DINA systems are −5.9 and −26.7 kJmol^{-1}, respectively, which are smaller than those of TNAD/HMX and TNAD/RDX systems. This indicates that the larger the ΔE (the intermolecular interaction energy), the better the compatibility of components of the system.

The relationship between the radial distribution function and compatibility

The function of $g_{AB}(r)$ is often used to denote radial distribution function (RDF). The definition of $g_{AB}(r)$ is as follows:

Table 5 Density (ρ) before and after MD simulation (g/cm^3) and its changes (β)

Blends	ρ_{before}	ρ_{after}	β
TNAD/DINA	1.73	1.53	11.56
TNAD/DNP	1.71	1.44	15.79
TNAD/RDX	1.81	1.56	13.81
TNAD/HMX	1.85	1.59	14.05

Table 6 Interaction energy (kJmol^{-1}) of TNAD and other energetic components

Blends	E_{total}(a.u.)	$E_{(1)TNAD}$(a.u.)	$E_{(2)}$ (a.u.)	ΔE
TNAD/DINA	−965.685	−644.471	−347.879	−26.7
TNAD/DNP	−641.273	−505.978	−141.235	−5.9
TNAD/RDX	−2299.5	−644.471	−1698.55	−43.5
TNAD/HMX	−2257.53	−644.471	−1650.32	−37.3

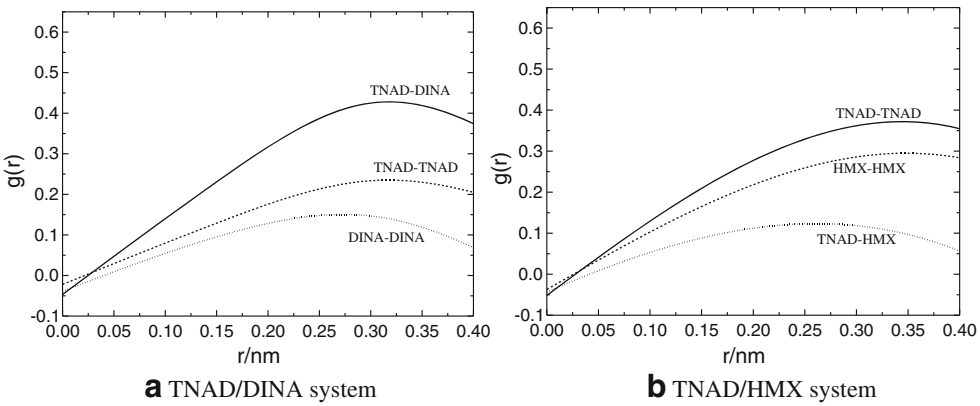

Fig. 4 Intermolecular RDF for TNAD/DINA **a** and TNAD/HMX **b** TNAD HMX RDX DNP DINA

a TNAD/DINA system **b** TNAD/HMX system

$$g_{AB}(r) = \frac{\langle n_{AB}(r) \rangle}{4\pi r^2 \Delta\rho_{AB}}. \quad (6)$$

RDF can show the interaction way among non-bond atoms. The interaction range of hydrogen bond ranges from 0.26 to 0.31 nm, the van der Waals interaction ranges from 0.31 to 0.50 nm. Figure 4 displays the RDF of TNAD/HMX and TNAD/DINA systems for comparison. From Fig. 4, the main interaction ways between TNAD and other energetic components are short-range interactions. In addition, $g_{AB}(r)$ is often used to judge the compatibility of blends. If the $g_{AB}(r)$ of the blend is much higher than the $g_{AB}(r)$ of the pure energetic component, the compatibility is better. On the contrary, the phase separation may happen [35–37]. From Fig. 4, it is noted that the $g_{AB}(r)$ graph of TNAD/DINA is much higher than those of pure TNAD and DINA, while the $g_{AB}(r)$ graph of TNAD/HMX is much lower than those of pure TNAD and HMX. This shows that the miscibility of TNAD/DINA system is much better than that of TNAD/HMX, which is consistent with the above conclusion.

Judged by the solubility parameter, density and RDF, the miscibility of TNAD/DINA is good while that of TNAD/DNP is poor. This conclusion is consistent with the experimental results of Yan et al. [9], which states the chemical compatibility. When the chemical compatibility of a binary system is good, there is no chemical reaction or the chemical reaction of the system is very weak, so the miscibility is also good and vice versa.

Conclusions

In this paper, the MD simulations using COMPASS force field were used to evaluate the miscibility of TNAD and other energetic materials. The analysis of solubility parameters shows that the order of miscibility is TNAD/DINA > TNAD/DNP > TNAD/RDX > TNAD/HMX, which is different from the order of the experimental results that derived from the comprehensive outcomes of chemical compatibility. The densities and binding energies of four blends were also calculated. It is noted that the miscibility between TNAD and the other energetic material becomes better with the decrease of the density change rate. The compatibility of components of the system becomes better with the augment of the intermolecular interaction energy. According to the analysis of RDF, the main interaction ways between TNAD and other energetic components are short-range interactions.

Acknowledgments We gratefully acknowledge the funding provided by the Laboratory of Science and Technology on Combustion and Explosion (Grant No. 9140C3501021101) for supporting this work.

References

1. Vogelsanger B (2004) Chemical stability, compatibility and shelf life ofexplosives. Chimia 58:401–408
2. Hildebrand JH, Scott RL (1950) The solubility of non-electrodytes. Reinhold, New York
3. Chang CS, Den TG (1997) Characterization and preparation of three new high energetic materials (TNAD. DNNC and HCO) Huaxue 55(2):89–106
4. Willier RL (1983) Propell Explos Pyro 8(3):65–69
5. Liu MS, Tsai HJ, Den TG (1992) Study on the preparation of highly energetic material trans-1,4,5,8-tetranitro-1,4,5,8-tetraaza-decalin. Huoyao Jishu 8(3):1–8
6. Qiu L, Xiao HM, Zhu WH, Xiao JJ, Zhu W (2006) Ab initio and molecular dynamics studies of crystalline TNAD (trans-1,4,5,8-tetranitro-1,4,5,8-tetraazadecalin). J Phys Chem B 110:10651–10661
7. Prabhakaran KV, Bhide NM, Kurian EM (1995) Spectroscopic and thermal studies on 1,4,5 8-tetranitro tetraaza decalin (TNAD) J Thermochem Acta, 249–258
8. Skare D, Croatia Z (1999) Tendencies in development of new explosives: heterocyclic, benzenoid-aromatic and alicyclic compounds. Kemija u Industriji 48(3):97–102
9. Yan QL, Li XJ, Zhang LY, Li JZ, Li HL, Liu ZR (2008) Compatibility study of trans-1,4,5,8-tetranitro-1,4,5,8-tetraazadecalin (TNAD) with some energetic components and inert materials. J HazardMater 160:529–534
10. Materials Studio 4.0 (2006) Accelrys, Inc: San Diego, CA
11. Mader CL (1998) Numerical Modeling of Explosives and Propellants (2nd edn) CRC, Boca Raton

12. Ou YX, Chen JJ (2005) The High Energy and Density Compounds, 1st edn. National Defense Industry Press, Beijing
13. Suceska M, Zeman S, Rajic M (2001) Theoretical prediction of TNAZ detonation properties. New trends in rersearch of energetic materials, in: Proceedings of the Fourth Seminar. Pardubice, Czech Republic
14. http://www.chemnet.com/India/Products/1,4dinitropiperazine/Suppliers-0-0.html
15. Sun H, Ren P, Fried JR (1998) The COMPASS forcefield: parameterization and validation for polyphosphazenes. Comput Theor Polym Sci 8:229–246
16. Sun H (1998) COMPASS: an ab initio forcefield optimized for condensed-phase application-overview with details on alkane and benzene compounds. J Phys Chem B 102:7338–7364
17. Chen XP, Yuan CA, Wong CKL, Zhang GQ (2011) Validation of forcefields in predicting the physical and thermophysical properties of emeraldine base polyaniline. Mol Simulat 37:990–996
18. Bunte SW, Sun H (2000) Molecular Modeling of Energetic Materials: The Parameterization and Validation of Nitrate Esters in the COMPASS Force Field. J Phys Chem B 104(11):2477–2489
19. Cui HL, Ji GF, Chen XR, Zhu WH, Zhao F, Wen Y, Wei DQ (2010) First-principle study of high-pressure behavior of solid β-HMX. J Phys Chem A 114:1082–1092
20. Andersen HC (1980) Molecular dynamics simulations at constant pressure and/or temperature. J Chem Phys 72(4):2384–2393
21. Berendsen HJC, Postma JPM, van Gunsteren WF (1984) Molecular dynamics with coupling to an external bath. J Chem Phys 81(8):3684–3690
22. Allen MP, Tildesley DJ (1987) Computer Simulation of Liquids. Clarendon, Oxford
23. Ewald PP (1921) Die Berechnung optischer und elektrostatischer Gitterpotentiale. J Annu Phys 64:253–287
24. Karasawa N, Goddard WA (1992) Force fields structures and properties of poly(vinylidene fluoride) crystals. Macromolecules 25:7268–7281
25. Sun XQ, Fan XW, Ju XH, Xiao HM (2007) Research methods on component compatibility of propellants. Chem Propell Polym Mater 5:30–36
26. Cady HH, Lanson AC, Cromer DT (1963) The crystal structure of α-HMX and a refinement of the structure of β–HMX. Acta Cryst 16:617–623
27. Zhao XP, Liu J, Sun J (2010) The molecular structure and gas formation enthalpy calculation of RDX. Comput Appl Chem 27(7):890–892
28. van Krevelen DW, Hoftyzer PJ (1990) Properties of polymers. Elsevier, Amsterdam
29. Ren YL, Chen SZ (1981) Study on concentrated solution of nitrocellulose- solubility parameters and system compatibility. Chinese J Explos Propell 1:9–16
30. Xiao JJ, Huang H, Xiao HM (2007) MD simulation study on the mechanical properties of HMX crystals and HMX/F2311 PBXs. Acta Chim Sinica 65:1746–1750
31. Radovan T, Alessandro C, Marco F (2004) Computer simulation of polypropylene/organoclay nanocomposites: Characterization of atomic scale structure and prediction of binding energy. Polym 45:8075–8083
32. Paolo C, Giulio S, Sabrina P (2008) Many-scale molecular simulation for ABS-MM T nanocomposites: upgrading of industrial scraps. Micropor Mesopor Mater 107:169–179
33. Zhu W, Xiao HM, Zhao F (2007) Molecular dynamics simulation of elastic properties of HMX/TATB composite. Acta Chim Sinica 65:1223–1228
34. Subhra M, Golok B, Nando K (1996) Mechanical and dynamic mechanical properties of miscible blends of epoxidized natural rubber and poly(ethylene-co-acrylic acid). Polym 37:5387–5394
35. Clancy TC, Putz M (2000) Mixing of isotactic and syndiotactic polypropylenes in the melt. Macromolecules 33(25):9452–9463
36. Akten ED, Mattice WL (2001) Monte carlo simulation of head-to-head, tail-to-tail polypropylene and its mixing with polyethylene in the melt. Macromolecules 34(10):3389–3395
37. Gestoso P, Brisson J (2003) Towards the simulation of poly(vinylphenol)/poly (vinylmethylether) blends by atomistic molecular modeling. Polym 44(8):2321–2329